Far East Journal of Electronics and Communications
Volume 8, Number 1, 2012, Pages 23-33
Available online at http://pphmj.com/journals/fjec.htm
Published by Pushpa Publishing House, Allahabad, INDIA

ANALYSIS OF A GAIN-COUPLED DOUBLE PHASE-SHIFT-CONTROLLED DISTRIBUTED FEEDBACK OPTICAL FILTER

A. Jafari and S. Bakkeshizadeh

Department of Physics
Faculty of Science
Urmia University
Urmia, P. O. Box 165, Iran
e-mail: a.jafari@urmia.ac.ir

Abstract

In this paper, we propose and analyze gain-coupled laser diodes (GC LDs) and a gain-coupled double phase-shift-controlled distributed feedback (GC-2PSC-DFB) optical filter. Our analysis is based on the transfer matrix method. It is showed that in a distributed feedback diode laser with gain coupling, we can have an enhanced peak in the Bragg wavelength. We also show that in a (GC-2PSC-DFB) optical filter the range of tuning, the Side-mode suppression ratio (SMSR) and the power of the transmittance peaks can be improved by increasing the pitch of grating.

1. Introduction

Gain-coupled laser diodes (GC LDs) are basically LDs with purely imaginary coupling coefficients, where the coupling is generated by the change in gain along the structure [1]. There are two methods that could be

Keywords and phrases: distributed feedback lasers, gain-coupled distributed feedback lasers, optical filters, double phase-shift-controlled.

Received August 16, 2011

used to implement the GC active sections. Both of which have been realized experimentally [2]-[4]. For the first method, the gain coupling is achieved by fabricating a second layer of grating on top of a grating in a DFB LD, thereby canceling out the effect of index coupling [2]. Owing to the direct modulation of the active layer thickness, the actual gain-coupling coefficient of this structure may fluctuate according to the strength of the injection current. The second method to realize a GC DFB LD is by fabricating a periodic variation of loss along the longitudinal axis. With such a loss variation structure, the strength of the gain coupling is not affected by any change in the injection current. However, owing to the additional loss, the loss-coupling structure results in a higher threshold current [5].

Dense wavelength-division-multiplexed (DWDM) systems are expected to become the key technology in realizing broadband communications networks [6], [7]. In DWDM optical filter network, a number of information channels are simultaneously transmitted through a single fiber, whereby each channel is carried by a different optical carrier wavelength. To isolate a single or, multiple information channels from the fiber at the receiving or routing node, wavelength-tunable optical filters become key components for DWDM networks. Semiconductor wavelength-tunable optical filters are especially suitable for integration with other optical devices used in the system, such as the laser diodes, semiconductor optical switches, photo detectors, and other passive planar waveguides [8]. A semiconductor wavelength-tunable optical filter is basically a laser diode that is biased slightly below threshold. When an optical signal with a wavelength close to the oscillation wavelength of the device is incident on the input, the signal is amplified and emitted at the output. By changing the injection current, the wavelength can be tuned accordingly by changing the refractive index of the active region. The important optical filter parameters include wide wavelength tuning range, narrow bandwidth, and high (SMSR). In 1992, Numai proposed the phase-shift-controlled (PSC) index-coupled DFB, where the gain and transmission wavelength were controlled independently by applying different injection currents to the multiple electrodes present in the structure [9]. This filter has a tuning range of 120 GHz (9.5Å) with a constant of 24.5 dB gain and the bandwidth of 12 to 13 GHz. An important parameter of DFB filters is the coupling coefficient κ, which measures the wave feedback capability due to the presence of the corrugation.

In this paper, we present the analysis of characteristics performance of a GC LD and wavelength-tunable filter structure. This structure has constructed by three active and two PSC sections, in which PSC sections are sandwiched between the active sections. This paper is organized as follows: Section 2 discusses the numerical model in which coupled-mode equations are solved based on the transfer matrix method. Section 3 includes the numerical results obtained for the proposed GC LDs and filter structure, and section 4 concludes the paper.

2. Theoretical Analyses

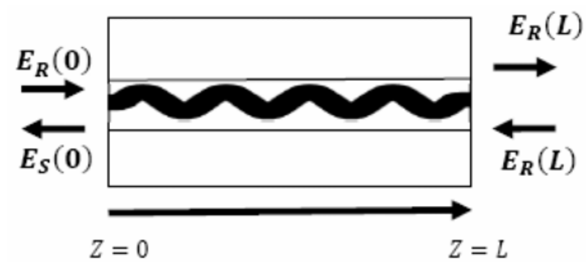

Figure 1. analytical model for DFB GC-LD.

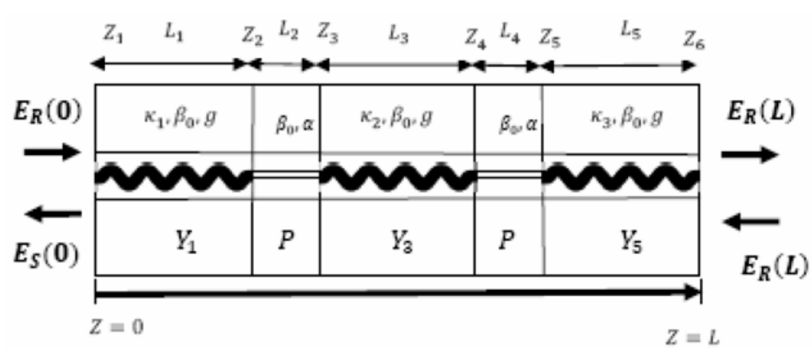

Figure 2. Proposed analytical model for GC-2PSC-DFB wavelength-tunable optical.

The analytical model for the GC LDs and DFB filter structures are shown in Figures 1 and 2, respectively. The complex amplitude of the electric field $E(z)$ inside the structures can be expressed as [10]:

$$E(z) = E_R(z) + E_S(z) = R(z)\exp(-j\beta_B z) + S(z)\exp(-j\beta_B z), \qquad (1)$$

where $E_R(z)$ and $E_S(z)$ are the normalized electric fields that propagate along opposite directions $R(z)$ and $S(z)$ are complex amplitudes of the forward and backward electric fields, respectively; $\beta_B = \frac{\pi}{\Lambda}$ is the Bragg frequency of the gratings and Λ is the grating period. According to the Maxwell equations, the following pair of coupled-mode equation could be obtained

$$-\frac{dR(z)}{dz} + (\alpha - j\delta)R(z) = j\kappa S(z), \qquad (2a)$$

$$\frac{dS(z)}{dz} + (\alpha - j\delta)S(z) = j\kappa R(z), \qquad (2b)$$

where α is the mode gain per unit length, $\delta = \beta - \beta_B$ is the detuning of the propagation constant, β, from the Bragg propagation constant, β_B, and κ is the grating coupling coefficient, which is governed by $\kappa = \kappa_n + j\kappa_g$; κ_n is the index-coupling coefficient and κ_g is the gain-coupling coefficient. For the proposed purely GC DFB structure, $\kappa_n = 0$ and thus, the coupling coefficient is reduced to $\kappa = j\kappa_g$.

From transfer matrix formalism point of view, the electrical fields, in the input and output surfaces of the structure, are related as [11]

$$\begin{bmatrix} E_R(z_{i+1}) \\ E_S(z_{i+1}) \end{bmatrix} = Y_i \begin{bmatrix} E_R(z_i) \\ E_S(z_i) \end{bmatrix} = \begin{bmatrix} y_{11} & y_{12} \\ y_{21} & y_{yy} \end{bmatrix} \begin{bmatrix} E_R(z_i) \\ E_S(z_i) \end{bmatrix}, \qquad (3)$$

where the input and output surfaces are defined as; z_i and z_{i+1}, respectively, the components of the matrix Y_i are given by

$$y_{11} = \frac{1}{1-\rho_i^2}\left(E_i - \frac{\rho_i^2}{E_i}\right)\exp[-j\beta_B(z_{i+1} - z_i)] \tag{4a}$$

$$y_{12} = \frac{\rho_i}{1-\rho_i^2}\left(E_i - \frac{1}{E_i}\right)\exp[-j\beta_B(z_{i+1} + z_i)] \tag{4b}$$

$$y_{21} = \frac{\rho_i}{1-\rho_i^2}\left(E_i - \frac{1}{E_i}\right)\exp[+j\beta_B(z_{i+1} + z_i)] \tag{4c}$$

$$y_{22} = \frac{1}{1-\rho_i^2}(E_i - \rho_i^2 E_i)\exp[j\beta_B(z_{i+1} - z_i)] \tag{4d}$$

with

$$E_i = \exp[\gamma_i(z_{i+1} - z_i)], \quad \rho_i = \frac{j\kappa_i}{(\alpha_i - j\delta_i) + \gamma_i}. \tag{5}$$

There also is a relation between complex amplitudes of the electrical fields, in the matrix formalism as [11]

$$\begin{bmatrix} R(z_{i+1}) \\ S(z_{i+1}) \end{bmatrix} = F_i \begin{bmatrix} R(z_i) \\ S(z_i) \end{bmatrix} = \begin{bmatrix} f_{11} & f_{12} \\ f_{21} & f_{22} \end{bmatrix} \begin{bmatrix} R(z_i) \\ S(z_i) \end{bmatrix}, \tag{6}$$

where

$$f_{11} = \cosh[\gamma_i(z_{i+1} - z_i)] + \frac{(\alpha_i - j\delta)(z_{i+1} - z_i)}{\gamma_i(z_{i+1} - z_i)}\sinh[\gamma_i(z_{i+1} - z_i)] \tag{7a}$$

$$f_{12} = -j\frac{\kappa(z_{i+1} - z_i)}{\gamma_i(z_{i+1} - z_i)}\sinh[\gamma_i(z_{i+1} - z_i)] \tag{7b}$$

$$f_{21} = j\frac{\kappa(z_{i+1} - z_i)}{\gamma_i(z_{i+1} - z_i)}\sinh[\gamma_i(z_{i+1} - z_i)] \tag{7c}$$

$$f_{22} = \cosh[\gamma_i(z_{i+1} - z_i)] - \frac{(\alpha_i - j\delta)(z_{i+1} - z_i)}{\gamma_i(z_{i+1} - z_i)}\sinh[\gamma_i(z_{i+1} - z_i)]. \tag{7d}$$

In the above equations, γ_i is the complex propagation constant that satisfies the following dispersion equation:

$$\gamma_i^2(\alpha_i - j\delta_i)^2 + \kappa_i^2. \tag{8}$$

Since there is no active section and no grating in the planar PSC section (i.e., $\alpha_i = 0$ and $\kappa_i = 0$), the transfer matrix for the electric field of this section can be simplified to,

$$\begin{bmatrix} E_R(z_{i+1}) \\ E_S(z_{i+1}) \end{bmatrix} = P_i \begin{bmatrix} E_R(z_i) \\ E_S(z_i) \end{bmatrix} = \begin{bmatrix} \exp(\varphi) & 0 \\ 0 & \exp(-\varphi) \end{bmatrix} \begin{bmatrix} E_R(z_i) \\ E_S(z_i) \end{bmatrix}, \tag{9}$$

where $\varphi = \gamma_P L_P - j\beta_0 L_P$, γ_P is the value of γ_i in the PSC section and L_P is the length of the PSC section. The amount of phase shift, Ω, introduced by the PSC section is given by [12]

$$\Omega = \mathrm{Im}(2\gamma_{PSC} L_{PSC}) = \frac{4\pi(n_a - n_P)L_P}{\lambda_B}, \tag{10}$$

where n_a and n_p are the effective refractive indices of the active and PSC sections, respectively and where λ_B refers to the Bragg wavelength. The value of n_p decreases as the current injection I_P into the PSC section increases; hence, according to equation (12), the value of Ω increases.

3. Results and Discussions

3.1. Enhanced gain in the distributed feedback diode lasers with gain coupling

The structure under study in this case was shown in Figure 1. An optical signal is injected into the structure and because of feedback, it is amplified and the result is appeared in the output. Equations (6), (7) are used for the theoretical study of this structure. We chose zero values for the reflectivity's of the both surfaces at z_1 and z_2. The injected signal power in the input, in P_{in}, and the amplified output power, P_{amp}, are proportional to the $|R(0)|^2$ and $|R(L)|^2$, respectively. The structure's parameters are defined as; $\kappa L = 4.83$, $L = 500\,\mu\text{m}$ and $\Lambda = 0.21\,\mu\text{m}$ and the gain of the signal, G, is given as:

$$G = \frac{P_{amp}}{P_{in}} = \left| \frac{R(L)}{R(0)} \right|^2 = \left| \frac{1}{f_{22}} \right|^2. \tag{11}$$

In Figure 3, the gain of the signal is depicted as a function of $\lambda - \lambda_B$ where λ is the injected signal wavelength. As it can be seen from this figure, on the contrast to the DFB diode lasers with index coupling, which have not any peak in the Bragg wavelength, the DFB diode lasers with gain coupling have an enhanced peak in the Bragg wavelength. This result that is obtained using the transfer matrix method is confirmed by the theory of the diode lasers with gain coupling, in which a signal oscillation mode in the Bragg wavelength has been predicted [1].

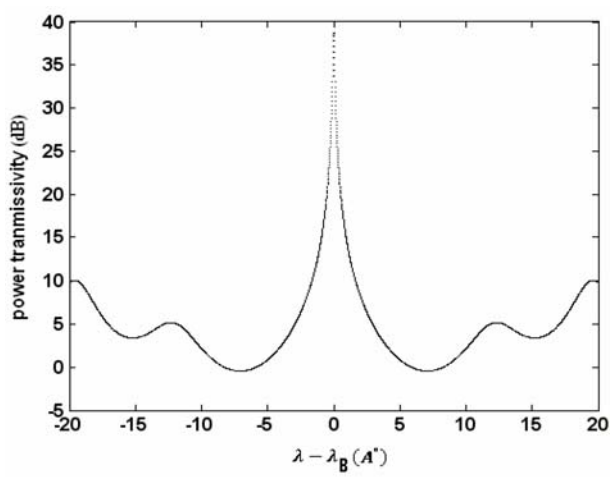

Figure 3. Calculated gain profiles of a DFB GC-LD in terms of relative wavelength $\lambda - \lambda_B$. Also $\kappa L = 4.83$, $\lambda_B = 1.55\,\mu\text{m}$, $L = 500\,\mu\text{m}$ and $\Lambda = 0.21\,\mu\text{m}$.

3.2. Gain-coupled double phase-shift-controlled distributed feedback optical filter

The structure of the studied optical filter was shown in Figure 2. This structure has constructed by three active and two phase-shift-controlled (PSC) sections, in which PSC sections are sandwiched between the active sections. The filter cavity is divided to five sections and its total transfer matrix is the production of the transfer matrixes of the layers and is defined as:

$$\begin{bmatrix} E_R(L) \\ E_S(L) \end{bmatrix} = Y_5 P Y_3 P Y_1 \begin{bmatrix} E_R(0) \\ E_S(0) \end{bmatrix} = \begin{bmatrix} T_{11} & T_{12} \\ T_{21} & T_{yy} \end{bmatrix} \begin{bmatrix} E_R(0) \\ E_S(0) \end{bmatrix}, \tag{12}$$

where, Y_i and P are the transfer matrixes of the active and PSC sections, respectively that are given by equations (4), (9). In equation (4), the origin and the length of the structures L, are specified as $z_1 = 0$ and $z_6 = L = \sum_{i=1}^{5} L_i$, respectively. The transmission power of the filter can be given as;

$$T = \left| \frac{E_S(L)}{E_R(0)} \right|^2 = \left| \frac{1}{T_{22}} \right|^2. \tag{13}$$

The threshold gain, α_{th}, and the detuning parameter, δ, could be obtained by solving the following equation;

$$T_{22}(\alpha_{th}, \delta) = 0. \tag{14}$$

Finally, the transmission power of the filter can be given by

$$T = \left| \frac{1}{T_{22}(\alpha = 0.98\alpha_{th}, \delta)} \right|^2. \tag{15}$$

A high output power and a bandwide lese than 10 dB can be obtained by $\alpha = 0.98\alpha_{th}$, so, this is the reason for this selection of the gain in equation (15) [13].

The transmissivity power of these filters has peaks at deferent wavelengths that are obtained under different values of phase shifts, Ω, given by equation (10).

The principal aim in these filters, is obtaining a wide tuning rang, by planning a structure with suitable parameters. In Figure 4, the tuning range of wavelength is plotted in terms of coupling coefficient at deferent grating pitches. It can be seen that, the tuning range of wavelength increase as the grating pitch increases. On that hand, maximum value of the tuning range was found at $\kappa_g = 4\text{mm}^{-1}$. So, in the following, we investigated the power transmissivity of the system only at $\Lambda = 0.21\,\mu\text{m}$ and $\kappa_g = 4\text{mm}^{-1}$.

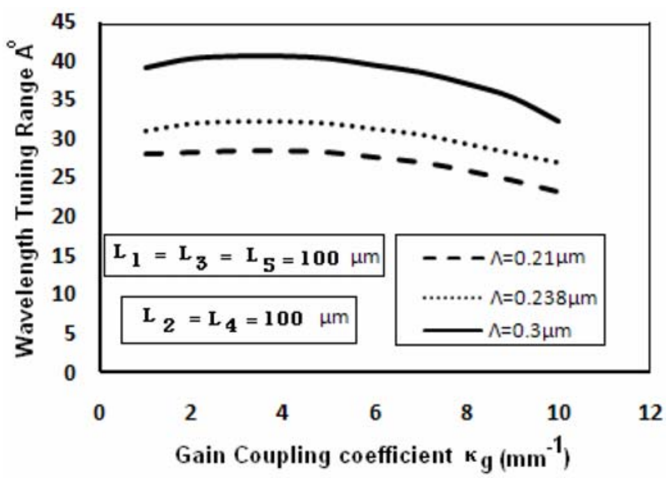

Figure 4. Variation of the wavelength tuning rang versus κ_g, ($\kappa_1 = \kappa_2 = \kappa_3 = \kappa_g$).

Figure 5 is plotted with $\kappa_g = 4\,\text{mm}^{-1}$, $\Lambda = 0.21\,\mu\text{m}$ and $L = 500\,\mu\text{m}$. The transmissivity power peaks have obtained under different Ωs. The oscillation mode in the Bragg wavelength is appeared at $\Omega_1 = \Omega_2 = \pi$ and a tuning range of $\Delta\delta = 0.0274\,\mu\text{m}^{-1}$ (correspond to $\Delta\lambda = 28.38\,\text{Å}$) which is occurred between $\Omega_1 = \Omega_2 = 0$ and 2π and is wider than predicted value in reference [9], [14]. The SMSR of modes is grater than 14 dB and the power of the transmittance peaks are higher than 45 dB for this structure.

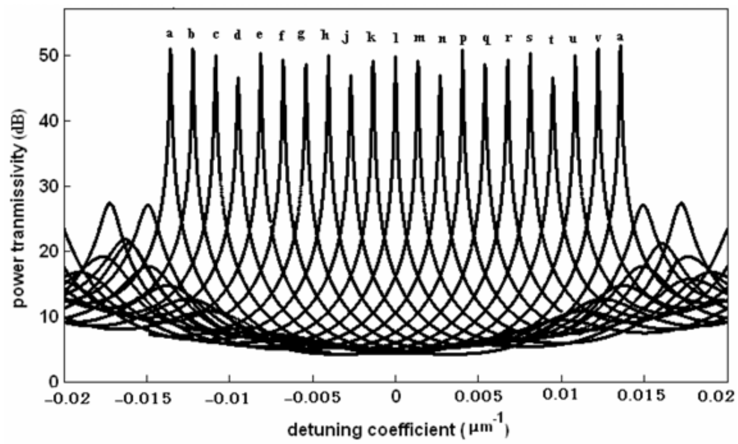

Figure 5. Power transmissivity versus detuning coefficient for different values of Ω from 0 to 1.9π in steps of 0.1π. Also, $\kappa_1 = \kappa_2 = \kappa_3 = \kappa_g = 4\text{mm}^{-1}$, $\lambda_B = 1.55\,\mu\text{m}$, and $\Lambda = 0.21\,\mu\text{m}$. With label l also representing $\Omega = \pi$.

4. Conclusions

The enhancement of the output power of a DFB LD with gain coupling, and the wavelength tuning rang, SMSR of the modes and the maximum peak transmissivity of a new GC-DFB wavelength-tunable filter structure have been studied. It was found that on the contrast to the DFB-LDs with index coupling, the DFB-LDs with gain coupling have an enhanced peak in the Bragg wavelength. It was also showed that our GC-DFB wavelength- tunable filter present a wide tuning rang with large SMSR. An almost power of the transmittance peaks higher than 45 dB, the SMSR of the modes more than 14 dB and a tuning range of 28.38 Å can be achieved using this structure. In particular, the effect of the grating pitch on improvement of the above characteristics of the filter has been studied.

References

[1] H. Kogelnik and C. V. Shank, Coupled-wave theory of distributed feedback lasers, J. Appl. Phys. 43 (1972), 2327-2335.

[2] Y. Luo, Y. Nakano, K. Ikeda, K. Tada, T. Inoue, H. Hosomatsu and H. Iwaoka, Low threshold CW operation in a novel gain-coupled distributed feedback semiconductor laser, Tech. Dig. 12th IEEE Int. Semiconductor Laser Conf., Davos, Switzerland, 1990, pp. 70-71.

[3] Y. Nakano, Y. Deguchi, K. Ikeda, Y. Luo and K. Tada, Resistance to external optical feedback in gain-coupled semiconductor DFB laser, Tech. Dig. 12th IEEE Int. Semiconductor Laser Conf., Davos, Switzerland, Sep. 1990, pp. 71-72.

[4] Y. Luo, Y. Nakano, K. Tada, T. Inoue, H. Hosomatsu and H. Iwaoka, Purely gain-coupled distributed feedback lasers, Appl. Phys. Lett. 56 (1980), 1620-1622.

[5] H. Ghafouri-Shiraz and B. S. K. Lo, Distributed Feedback Laser Diodes: Principles and Physical Modeling, Wiley, New York, 1996, pp. 148-149.

[6] S. Suzuki and K. Nagashima, Optical broadband communications network architecture utilizing wavelength-division switching technology, Photonic Switching, T. K. Gustafson and P. W. Smith, eds., Springer-Verlag, Berlin, Germany, 1998, pp. 134-137.

[7] C. A. Brackett, Dense wavelength division multiplexing networks: principles and applications, IEEE J. Sel. Areas Commun. 8 (1990), 948-964.

[8] T. Numai, Semiconductor tunable wavelength filters, Presented at the Third Optoelectronic Conf.: Invited Talk, Chiba, Japan, 1990.

[9] T. Numai, 1.5 μm phase-shift-controlled distributed feedback wavelength tunable optical filter, IEEE J. Quantum Electron. 28 (1992), 1513-1519.

[10] H. Kogelnik and C. V. Shank, Coupled-wave theory of distributed feedback lasers, J. Appl. Phys. 43 (1972), 2327-2335.

[11] H. Ghafouri-Shiraz and B. S. K. Lo, Distributed Feedback Laser Diodes: Principles and Physical Modeling, Wiley, New York, 1996, pp. 257-260.

[12] H. Ghafouri-Shiraz and B. S. K. Lo, Distributed Feedback Laser Diodes: Principles and Physical Modeling, Wiley, New York, 1996, pp. 268-269.

[13] K. Magari, H. Kawaguchi, K. Oe and M. Fukuda, Optical narrowband filters using optical amplification with distribute feedback, IEEE J. Quantum Electron. 24 (1988), 2178-2190.

[14] Kian Yong Lim and L. Y. Andy Low, Su Fong Chien and H. Ghafouri-Shiraz, Tunable optical narrowband filter using a gain-coupled phase-shift-controlled distributed feedback laser, IEEE J. Quantum Electron. 11 (2005), 913-918.